Physica B 407 (2012) 2841–2845

Contents lists available at SciVerse ScienceDirect

Physica B

journal homepage: www.elsevier.com/locate/physb

First principles study of O defects in CdSe

J. T-Thienprasert [a,b], S. Limpijumnong [c,d,*], M.-H. Du [d], D.J. Singh [d]

[a] Department of Physics, Kasetsart University, Bangkok 10900, Thailand
[b] Thailand Center of Excellence in Physics (ThEP Center), Commission on Higher Education, Bangkok 10400, Thailand
[c] School of Physics, Suranaree University of Technology and Synchrotron Light Research Institute, Nakhon Ratchasima 30000, Thailand
[d] Oak Ridge National Laboratory, Oak Ridge, TN 37831, USA

ARTICLE INFO

Available online 24 August 2011

Keywords:
Infrared spectroscopy
First-principles calculations
Defect
Local vibration modes
CdSe
Dynamic matrix

ABSTRACT

Recently, the vibrational signatures related to oxygen defects in oxygen-doped CdSe were measured using ultrahigh resolution Fourier transform infrared (FTIR) spectroscopy by Chen et al.(2008) [1]. They observed two absorption bands centered at ~1991.77 and 2001.3 cm^{-1}, which they attributed to the LVMs of O_{Cd}, in the samples grown with the addition of CdO and excess Se. For the samples claimed to be grown with even more excess Se, three high-frequency modes (1094.11, 1107.45, and 1126.33) were observed and assigned to the LVMs of O_{Se}–V_{Cd} complex. In this work, we explicitly calculated the vibrational signatures of O_{Cd} and O_{Se}–V_{Cd} complex defects based on first principles approach. The calculated vibrational frequencies of O_{Cd} and O_{Se}–V_{Cd} complex are inconsistent with the frequencies observed by Chen et al., indicating that their observed frequencies are from other defects. Potential defects that could explain the experimentally observed modes are suggested.

1. Introduction

Distinct local vibrational modes (LVMs) in oxygen-doped CdSe have been experimentally observed by Chen et al. using Fourier transform infrared (FTIR) spectroscopy [1]. In their work, the CdSe crystal was grown with the addition of CdO to provide oxygen and excess Se to suppress the formation of Se vacancies. Using FTIR, they found two absorption bands centered at ~1991.77 and 2001.3 cm^{-1}, which they assigned to the LVM of substitutional oxygen on Cd site (O_{Cd}) [1]. For samples with even higher level of excess Se, they observed three lower frequency modes at 1094.11, 1107.45, and 1126.33 cm^{-1}, which they assigned to the LVMs of substitutional oxygen on Se site complexing with a Cd vacancy (O_{Se}–V_{Cd}) [1]. The absorption bands of around 1100 cm^{-1} have also been reported by the same group in the case of O doped CdTe, and in a similar manner, were assigned to the LVMs of substitutional oxygen on Te site complexing with a Cd vacancy (O_{Te}–V_{Cd}) [2,3]. Generally, the LVMs of defects containing a single oxygen atom would have vibration frequencies well below 1000 cm^{-1}. To investigate these defects, we employed first principles approach based on density functional theory to calculate their stability and LVMs.

Our calculated results show that the vibration frequencies of O_{Se}–V_{Cd} are ~495 cm^{-1} for the high frequency modes and 201 cm^{-1} for the low frequency mode. Because the observed values by Chen et al. [1] are significantly higher (~ 1100 cm^{-1}), O_{Se}–V_{Cd} cannot be the cause of these observed absorption bands. Our calculations also showed that the observed higher absorption bands (around 2000 cm^{-1}) in some of Chen et al.'s samples cannot come from O_{Cd} for at least two reasons: (1) the defect has a very high formation energy, i.e., over 2 eV higher than O_{Se} even under Se-rich condition. It is also energetically unstable against spontaneous transformation into O_{Se}–Se_{Cd}. (2) Even if O_{Cd} is metastable, its frequencies are all below 730 cm^{-1} (the O_{Se}–Se_{Cd} complex also has frequencies all below 420 cm^{-1} [4]).

In this paper, we report our detailed results on the energetic and LVM calculations of the O-related defects in CdSe based on first principles density functional theory. Because CdSe has a wurtzite crystal structure, the defects have less degenerate modes compared to their counterparts in CdTe, which has a zincblende structure [5]. The paper is organized as follows. In Section 2, we describe the detailed computational method and parameters used in the first principles calculations. In Section 3, the formation energy and structure of each defect are discussed. The relevant LVMs are reported and discussed in comparison with the experimental results. Potential defects that might have LVM in accordance with the measured results are suggested. Last, in Section 4, we summarize our main results.

2. Calculation methods

In this work, the density functional theory (DFT) within the local density approximations (LDA) was utilized. For the electron–ion interactions the ultra-soft pseudopotentials (USPP) [6], as

* Corresponding author at: School of Physics, Suranaree University of Technology, Nakhon Ratchasima 30000, Thailand. Tel.: +66 44 22 4319. fax: +66 44 22 4185.
E-mail address: sukit@sut.ac.th (S. Limpijumnong).

0921-4526/$ - see front matter © 2011 Elsevier B.V. All rights reserved.
doi:10.1016/j.physb.2011.08.042

implemented in the VASP code [7,8], were used. The use of USPP leads to a relatively smooth wave function; allowing us to use a relatively low energy cutoff for plane wave basis set (400 eV). The calculated lattice parameters of $a=4.290$ Å and $c=6.915$ Å are in good agreement with prior computation results [9,10] and are in a reasonable agreement with the experimental values of $a=4.300$ Å and $c=7.011$ Å [11].

To study defects, we used a supercell approach [12] with a 96-atom wurtzite supercell (described in Ref. [13]) and a Monkhorst–Pack [14] sampling k-points mesh of $2\times2\times2$. For each defect, all atoms in the supercell were allowed to relax until the (Hellmann-Feynman) forces [15] were reduced below 10^{-3} eV/Å. To determine the chance of formation and the stability of each defect, we calculated defect formation energy, which is defined as [16,17]

$$\Delta H_f = E_{tot}(D^q) - E_{tot}(0) + \sum \Delta n_x \mu_x + q(E_F + E_v), \quad (1)$$

where $E_{tot}(D^q)$ is the calculated total energy of a supercell containing a defect D in charge state q, $E_{tot}(0)$ is the calculated total energy of the same supercell without any defect, Δn_x is the number of atoms in species X (here, X can be Cd, Te, or O) being added into (negative sign if being removed) a defect-free supercell to create a supercell with defect D. μ_x is the chemical potential of the reservoir of X, E_F is the electron Fermi energy of the system referenced to the valence band maximum (VBM), and E_v is the VBM at the special k-point.

To grow CdSe in equilibrium, the following condition is also required:

$$\mu_{CdSe} = \mu_{Cd} + \mu_{Se}, \quad (2)$$

where μ_{CdSe} is the chemical potential of CdSe crystal. Our calculated heat of formation per molecular formula of CdSe is $\Delta H = \mu_{CdSe} - \mu_{Cd} - \mu_{Se} = -1.16$ eV in reasonable agreement with the previous works [18,19]. When additional element is added into the system, in this case O, other phase precipitation limits have to be taken into consideration. Because CdO is very stable, its formation defines the equilibrium precipitation limit for O. The highest chemical potential of oxygen under equilibrium growth should be $\mu_O = \mu_{CdO} - \mu_{Cd}$.

To study the LVMs of O-related defects in CdSe, i.e., O_{Cd}, O_{Se}, and O_{Se}–V_{Cd}, we used a so-called frozen phonon approach [5]. Based on the approach, both the vibrational frequency (eigenvalue) and the movement vectors of all atoms (eigenvector) of each mode are obtained. The frequencies obtained for various systems of defects in semiconductors by this approach are in good agreement with the experiments [20–26].

3. Results and discussions

The calculated wurtzite CdSe has the vertical and in-plane bonds slightly different with the vertical bond slightly longer (2.617 Å vs 2.615 Å) as illustrated in Fig. 1(a). The calculated direct band gap at Γ-point is 0.51 eV, which is smaller than the experimental value of 1.74 eV [27] due to the well-known DFT band gap underestimation. Note, however, that for the defects calculations, the band gap at the sampling k-points is 1.62 eV.

To investigate the models for oxygen defects in CdSe, especially those proposed by Chen et al. [1], we employed the supercell approach using a 96-atom supercell. The fully relaxed local structures of studied defects are shown using the ball and stick model in Fig. 1. Fig. 2 showed their formation energies as a function of Fermi-level (E_F) under two growth conditions (Cd-rich and Se-rich).

For O_{Se}, which is an isovalent substitutional, the formation energy of this defect is low indicating relatively high concentration. In general, one might expect O_{Se} to form easily under Cd-rich, i.e., Se-poor, conditions. However, when the CdO phase precipitation limit ($\mu_{Cd}+\mu_O=\mu_{CdO}$) is assumed, the formation energy of O_{Se} becomes independent of μ_{Cd}. Therefore, our calculated formation energy of O_{Se} is the same for both Cd- and Se-rich conditions. The local structure (Fig. 1c) shows that all four Cd atoms contract closer to the O atom to form Cd–O bonds with a

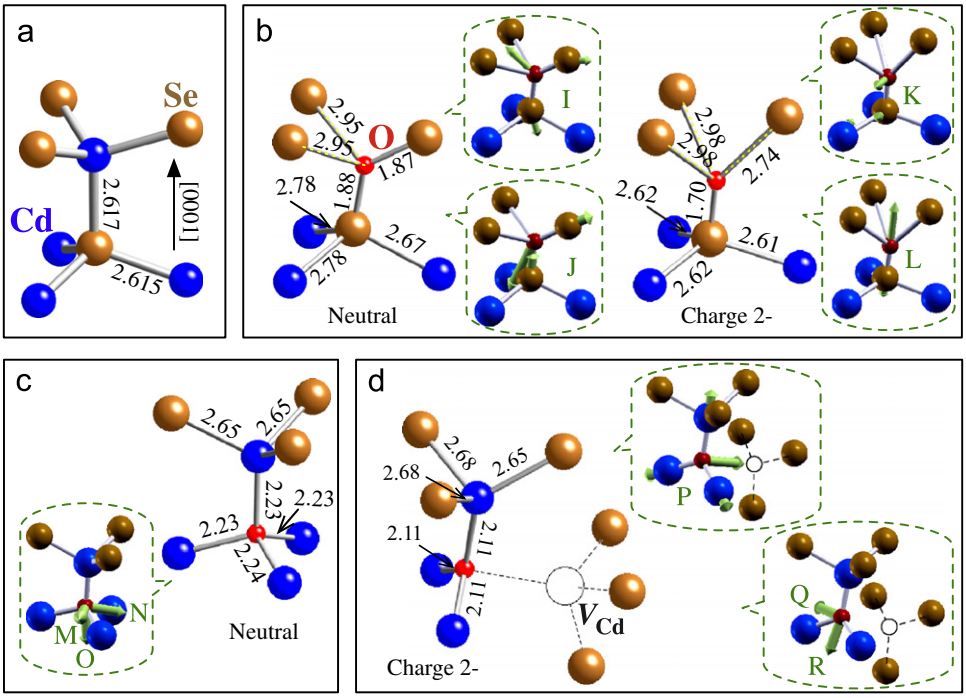

Fig. 1. The ball and stick models represent calculated local structures of bulk and oxygen defects in CdSe. (a) Bulk CdSe, (b) O_{Cd} in neutral and 2– charge states, (c) O_{Se} in the neutral charge state, and (d) O_{Se}–V_{Cd} complex in 2– charge state. The numbers indicate the computational bond distances in angstrom. The insets illustrate the eigenvectors of the localized modes (labeled I to R in accordance with Fig. 3). Only large components are shown. Modes M, N, and O (as well as Q and R) are shown in the same inset and small components of the neighbors are omitted.

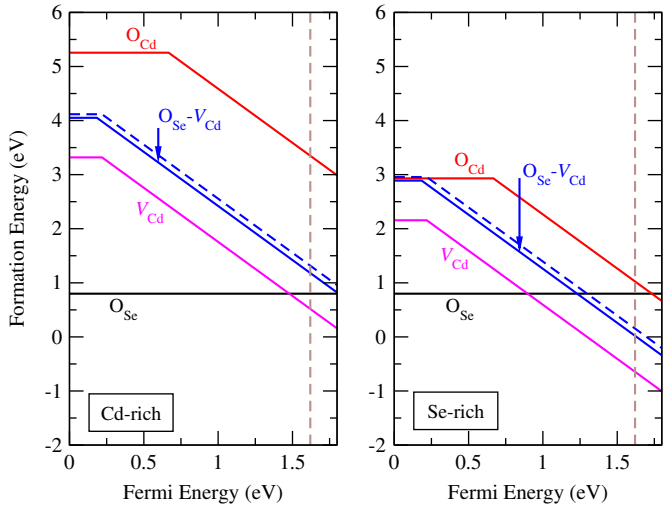

Fig. 2. Formation energies as a function of Fermi energy of defects in CdSe under Cd-rich (left) and Se-rich (right) conditions. The slope of each line indicates the defect's charge state. The dashed (blue) line is the sum of V_{Cd} and O_{Se} formation energies. The vertical dashed line indicated the calculated band gap.

distance of 2.23 Å, which is similar to Cd–O bond distance in CdO (computation: 2.32 Å, experiment: 2.35 Å). To accommodate the contraction, the bonds between each of the four Cd atoms and its three Se neighbors are slightly extended by 1.3% to 2.65 Å. Note that, in Fig. 1c, the slightly larger numerical value (2.24 Å) of one of the three Cd–O non-axial (not along the *c*-axis) bonds is actually due to inter-supercell interactions. Although, an isolated O_{Se} has three-fold symmetry, the 96-atom supercell (which has a rectangular prism cell shape) does not. This leads to a slight C_{3v} symmetry breaking in the supercell calculations.

Unlike an isovalent O_{Se}, which is a low energy and electrically neutral defect, the anti-site O_{Cd} has high formation energy due to mismatches in both atomic size and valence electrons. Even under the most favorable growth conditions, i.e., Se-rich, the formation energy of the neutral charge O_{Cd} remains at almost 3 eV, indicating low concentration. O_{Cd} is a very deep double acceptor with a transition level at $\varepsilon(0/2-)=0.67$ eV as shown in Fig. 2. However, the defect is thermally unstable against the reaction $O_{Cd}\rightarrow O_{Se}$–$Se_{Cd}+0.96$ eV, i.e., the O atom switches its site with one of its neighboring Se and the energy released in the process is 0.96 eV. Although, the energetic determinations alone already showed that O_{Cd} should not be the cause of the absorption bands of $\sim$2000 cm^{-1} observed by Chen et al., we performed further calculations to show that O_{Cd} by no means can give the vibration frequency that high. In the neutral charge state, the O atom is located off center, binding strongly with two Se atoms, one axial (along the *c*-axis) and one non-axial, with the bond distances of $\sim$1.9 Å. The other two O–Se bonds are basically broken with the distance of 2.95 Å, indicated by (yellow) dashed lines in Fig. 1b. In the 2− charge state, the O atom binds strongly with only one Se atom—the one along the principal axis, with the bond distance of 1.7 Å. The other three O–Se bonds are broken with the distance of 2.98, 2.98, and 2.74 Å, indicated by (yellow) dashed lines. Our results will show that the defect in both charge states has LVM frequencies that are all well below 2000 cm^{-1}.

To examine the O_{Se}–V_{Cd} complexes' defects, a Cd neighbor of the O_{Se} center was removed. Due to symmetry, there are two slightly different configurations of O_{Se}–V_{Cd} complex, i.e., there are two different types of Cd neighbors that can be removed: (1) the axial Cd neighbor sitting on top of O_{Se} or (2) one of the three non-axial Cd neighbors. Here, we focus our attention only on the non-axial configuration (Fig. 1d) because the axial configuration is $\sim$0.1 eV higher in energy. (We do not expect the axial configuration to yield very different LVM anyway). In Fig. 1d, the oxygen atom forms three strong bonds with its three Cd neighbors with the bond distance of 2.11 Å. The O_{Se}–V_{Cd} complex is a double acceptor with high formation energy under p-type conditions as shown in Fig. 2. To determine the stability of this complex, the binding energy was determined according to the reaction: $O_{Se}+V_{Cd}\rightarrow O_{Se}$–$V_{Cd}+E_b$. The calculated formation energies of O_{Se}, V_{Cd}, and O_{Se}–V_{Cd} complex are shown in Fig. 2 along with the sum of O_{Se} and V_{Cd} formation energies (dashed line). We obtained a small positive binding energy of only 0.13 eV.

To compare with the experimental results [1], the LVMs of O-related defects, i.e., O_{Cd}, O_{Se}, and O_{Se}–V_{Cd}, were calculated using the full dynamic matrix approach. Each defect is allowed to relax fully before each atom is displaced in *x*, *y*, and *z* direction one-at-a-time by a small distance in both positive and negative directions ($96\times3\times2=576$ calculations for each defect) to record the force responses on all atoms and to construct the force matrix. Then all $96\times3=288$ LVMs describing all possible modes of the 96-atom supercell containing the defect are calculated. To identify the modes that are localized on the O atom, we calculated the "localization" [28,29] defined as the sum-square of three eigenvector components (i.e., *x*, *y*, and *z*) on the O atom in each mode, denoted as $\sum u_0^2$. Because, for each mode, the sum-square of all atoms is normalized to unity, the theoretical highest possible value for $\sum u_0^2$ is 1 (perfectly localized) and the theoretical lowest possible value is 0 (not involved in the vibration mode). For each defect, the $\sum u_0^2$ of all modes is shown in the histogram style according to the frequency of the LVM in Fig. 3. The modes with large $\sum u_0^2$ are the modes that are localized on the O atom.

Because the two charge states of O_{Cd} have distinctive local structures, the LVMs of both structures are different. For O_{Cd}^0, the O atom bonds strongly with two Se atoms forming a bridge configuration as shown in Fig. 1b. The calculations give two localized modes at 417 cm^{-1} and 502 cm^{-1}, labeled I and J in Fig. 3a with the eigenvectors illustrating the relative amplitudes and directions of vibrations in the inset of Fig. 1b. For mode I, the three atoms (two Se and an O) vibrate such that both Se–O bonds are simultaneously stretched and then compressed. For mode J, the three atoms vibrate in a way such that one Se–O bond is stretched while another bond is compressed. These modes are similar to the symmetric and anti-symmetric stretch modes of a water molecule. The values of $\sum u_0^2$ are 0.85 and 0.91, reflecting a strong localization. Other lower frequencies modes (wag, rotation, translation modes) are coupled strongly with the host and are not very localized on O. These modes are noticeable in the region of 100–160 cm^{-1}. For O_{Cd}^{2-}, the O atom bonds strongly with only one Se atom as shown in Fig. 1b. For this configuration, the calculations give a localized ($\sum u_0^2=0.85$) mode at 723 cm^{-1}, labeled L. The eigenvectors for this L mode (inset of Fig. 1b) clearly show that it is the Se–O bond stretching mode. Among the lower frequencies modes, there is only one mode that shows some degree of localization ($\sum u_0^2=0.57$). It is the wag mode of the O atom, labeled K in Fig. 3b and inset of Fig. 1b. The frequency of the mode is 158 cm^{-1}. While our results on the formation energies already show that O_{Cd} is not stable and should not form in CdSe, the LVM calculations here further show that even if the O_{Cd} can form they would not give the high frequency modes responsible for the 2000 cm^{-1} absorption bands observed by Chen et al. The high frequency bands (1991.77 and 2001.3 cm^{-1}) observed by Chen et al. must be associated with other defects. The potential candidates are those containing Se–H bonds.

For isovalent substitution O_{Se}, the local structure is quite simple, i.e., the O atom forms short bond with surrounding Cd in a similar manner as O_{Te} in CdTe [5]. The calculations show three strong localized modes on O atom at 377, 379, and

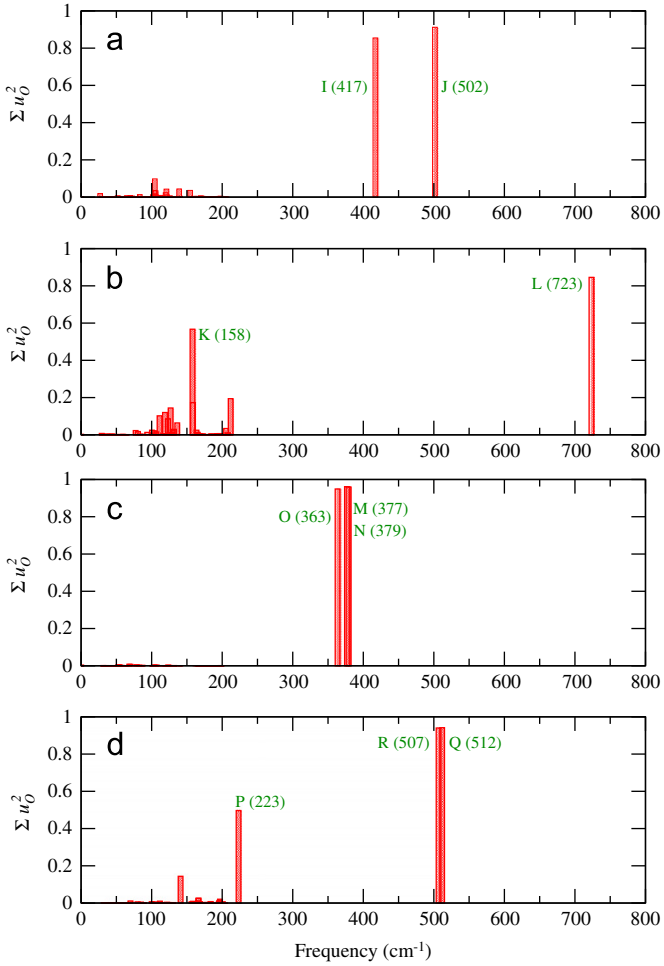

Fig. 3. Localization plots (sum-square of three eigenvector components on the O atom, $\sum u_0^2$) for all vibrational modes obtained using a 96-atom CdSe supercell of (a) O_{Cd} in the neutral charge state, (b) O_{Cd} in the 2– charge state, (c) O_{Se}, and (d) O_{Se}–V_{Cd} complex. The letters (I to R) indicate the modes that are localized on the O atom. Their associated eigenvectors are illustrated in the insets of Fig. 1. The numbers in parentheses indicate the frequencies in cm^{-1}.

363 cm^{-1} with $\sum u_0^2 = 0.96, 0.96$,and 0.95, respectively. The modes are labeled by M, N, and O in Fig. 3c. These modes can be described by the vibrations of the O atom in the axial (parallel to *c*-axis) direction (363 cm^{-1}) and two non-axial directions perpendicular to the first vibrational direction. As already mentioned, because of the choice of the supercell used for the calculations, the two, otherwise degenerate, non-axial modes (labeled M and N) are split. We shall take the average value of 378 cm^{-1} as the characteristic of the degenerate non-axial mode. These calculated values 363 cm^{-1} (axial) and 378 cm^{-1} (non-axial) are in a good agreement with Chen et al.'s estimated absorption bands for O_{Se} of 350–450 cm^{-1} [1]. In the inset of Fig. 1c, we present the eigenvector of all three localized modes (M, N, and O) in the same bond and stick crystal model because the vibration is really dominated by only the O atom moving in three different directions. Note that for CdTe, which has higher (cubic) symmetry, all three modes of O_{Te} are degenerated and have a comparable value (calculation: 338 cm^{-1} [5] and measurement: 350 cm^{-1} [2]) to the case at hand.

For O_{Se}–V_{Cd} defect complex, the O_{Se} atom largely shifts from the original Se site in the direction away from V_{Cd} such that the O stays almost in the plane formed by the three remaining Cd (see Fig. 1d). This leads to short Cd–O bonds (2.11 Å). As a result, the vibrational modes associated with the O vibrating in the plane of three Cd atoms have higher frequency than those of isolated O_{Se}. Our calculations found these two modes, labeled Q and R in Fig. 3d, to have frequencies 512 and 507 cm^{-1} and very localized with $\sum u_0^2 =$ 0.94. The two modes are shown in the inset of Fig. 1d. For the out-of-plane vibration (the direction perpendicular to the first two modes, involving the O atom vibrating in the direction of the V_{Cd}), the frequency is much lower at 223 cm^{-1}, labeled P in the inset of Fig. 1d. The mode is less localized with $\sum u_0^2 = 0.50$ due to stronger coupling with crystal phonon. These three modes can be roughly viewed as the splitting of the O_{Se} after being perturbed by the V_{Cd}. The three original O_{Se} LVMs of ~370 cm^{-1} are split into two high frequency modes (507 and 512 cm^{-1}) and one low frequency mode (223 cm^{-1}). These calculations show that the vibration frequencies of the O_{Se}–V_{Cd} defect complex is consistent with what to be expected based on the LVMs of isolated O_{Se}. These LVMs of O_{Se}–V_{Cd} defect complex have frequencies that are much smaller than the observed 1100 cm^{-1} absorption bands. Therefore, the O_{Se}–V_{Cd} defect complex cannot be the cause of the 1100 cm^{-1} absorption bands as Chen et al. have assigned. The absorption bands are likely related to the hydrogen defects, especially the frequency of around 1100 cm^{-1} were reported for the O–H wagging modes in CdTe as well as in other semiconductors [24,30]. Moreover, one should not rule out the diatomic molecules such as interstitial O_2, $(O_2)_{Te}$, $(O_2)_{Te}$–V_{Cd} complex, or O_2–V_{Cd} complex. Recently, O_2–V_{Cd} complex has been reported [31] to have a frequency in agreement with the observed 1100 cm^{-1} modes in CdTe [2]. However, its energetic stability as well as the oscillator strength that are important factors to explain the observed modes were not well discussed in details. To aid identification of these defects, it would be very useful to have additional data from different characterization techniques preferably the elemental selective ones. In this regard, x-ray absorption spectroscopy (in the oxygen *K*-edge region) would be highly suitable because it will help to pin point if the defects really contain O. If it does, the results will provide structural information as well as an oxidation state. However, this is a highly challenging task, which likely requires bright and highly collimated x-ray from advanced synchrotron facilities due to a low concentration of defects.

4. Conclusion

The oxygen defects in CdSe, namely O_{Cd}, O_{Se}, and O_{Se}–V_{Cd}, were studied based on first-principles density functional theory. Both energetic and vibration properties of these defects were calculated to determine their stabilities and local vibrational mode signatures. We concluded that the assignments of the infrared absorption bands at around 2000 cm^{-1} and 1100 cm^{-1} to O_{Cd} and O_{Se}–V_{Cd}, respectively, by Chen et al. [1] are incorrect. Our calculations showed that O_{Cd} has high formation energy and is energetically unstable, making it unlikely to form. Even if it is formed, its vibration signature should appear as absorption bands at 417 and 502 cm^{-1} or 158 and 723 cm^{-1}, depending on its charge state. All these frequencies are much lower than the observed ~2000 cm^{-1} absorption bands. For the O_{Se}–V_{Cd} complex, its vibration signature contains three localized frequencies of 223, 507, 512 cm^{-1}, which are, again, much lower than the observed ~1100 cm^{-1} absorption bands. We proposed that the absorption bands of around 2000 cm^{-1} are associated with defects containing Se–H bonds and the ones around 1100 cm^{-1} are associated with O–H complexes or O_2 related defects.

Acknowledgments

This work is supported by Thailand Research Fund (Grant no. RTA5280009) and National Nanotechnology Center (NANOTEC),

NSTDA, Ministry of Science and Technology, Thailand, through its program of Center of Excellence Network. Work at ORNL was supported by the US Department of Energy, Division of Materials Sciences and Engineering.

References

[1] G. Chen, et al., Phys. Rev. Lett. 101 (2008) 195502.
[2] G. Chen, et al., Phys. Rev. Lett. 96 (2006) 035508.
[3] G. Chen, et al., Phys. Rev. B 75 (2007) 125204.
[4] L. Zhang, et al., Phys. Rev. Lett. 102 (2009) 209601.
[5] J. T-Thienprasert, et al., Comput. Mater. Sci. 49 (2010) S242.
[6] G. Kresse, D. Joubert, Phys. Rev. B 59 (1999) 1758.
[7] G. Kresse, J. Furthmüller, Comput. Mater. Sci. 6 (1996) 15.
[8] G. Kresse, J. Hafner, J. Phys. Condens. Matter 6 (1994) 8245.
[9] K. Sarasamak, et al., Phys. Rev. B 77 (2008) 024104.
[10] K. Sarasamak, S. Limpijumnong, W.R.L. Lambrecht, Phys. Rev. B 82 (2010) 035201.
[11] F. Widulle, et al., Physica B 263–264 (1999) 448.
[12] C.G. Van de Walle, J. Neugebauer, J. Appl. Phys. 95 (2004) 3851.
[13] C.G. Van de Walle, S. Limpijumnong, J. Neugebauer, Phys. Rev. B 63 (2001) 245205.
[14] H.J. Monkhorst, J.D. Pack, Phys. Rev. B 13 (1976) 5188.
[15] R.P. Feynman, Phys. Rev. 56 (1939) 340.
[16] J.E. Northrup, S.B. Zhang, Phys. Rev. B 50 (1994) 4962.
[17] S.B. Zhang, J.E. Northrup, Phys. Rev. Lett. 67 (1991) 2339.
[18] R. de Paiva, R. Di Felice, ACS Nano 2 (2008) 2225.
[19] L. Manna, et al., J. Phys. Chem. B 109 (2005) 6183.
[20] M.-H. Du, S. Limpijumnong, S.B. Zhang, Phys. Rev. B 72 (2005) 073202.
[21] X. Li, et al., Appl. Phys. Lett. 86 (2005) 122107.
[22] X.-B. Li, et al., Phys. Rev. B 78 (2008) 113203.
[23] S. Limpijumnong, et al., Appl. Phys. Lett. 86 (2005) 211910.
[24] S. Limpijumnong, J.E. Northrup, C.G. Van de Walle, Phys. Rev. B 68 (2003) 075206.
[25] S. Limpijumnong, et al., Phys. Rev. B 77 (2008) 195209.
[26] S. Limpijumnong, C.G. Van de Walle, Phys. Rev. B 68 (2003) 235203.
[27] K. Woo-Chul, et al., Nanotechnology 18 (2007) 205702.
[28] A. Carvalho, et al., Phys. Rev. B 73 (2006) 245210.
[29] D. West, S.K. Estreicher, Phys. Rev. Lett. 96 (2006) 115504.
[30] M.-H. Du, H. Takenaka, D.J. Singh, Phys. Rev. B 77 (2008) 094122.
[31] W. Cheng, et al., Ann. Phys. (Berlin) 523 (2010) 129.